Hsa_circ_0043603 promotes the progression of esophageal squamous cell carcinoma by sponging miR-1178–3p and regulating AADAC expression

Xuezhong Wang [*], Zhiguang Liu, Yalong Du, Shuguang Hao, Bing Zhao

Department of Thoracic Surgical Oncology Ward One, Xinxiang Central Hospital, The Fourth Clinical College of Xinxiang Medical University, Xinxiang, Henan, 453003, China

ABSTRACT

This study aims to investigate the regulatory impact of hsa_circ_0043,603, a circular RNA, on the progression of esophageal squamous cell carcinoma (ESCC), which ranks as the sixth leading cause of global mortality.

We evaluated the expression, origin, and localization of hsa_circ_0043,603 in ESCC tumors using qRT-PCR, bioinformatics, and FISH analysis. Functional studies were conducted by manipulating the hsa_circ_0043,603 expression in Eca109 cells through overexpression and silencing plasmids. Additionally, xenografts derived from circ_0043,603-overexpressing Eca109 cells enabled us to investigate tumor growth, proliferation, and apoptosis. Through Starbase analysis, we identified miR-1178–3p as a target of circ_0043,603, which was validated using RIP and luciferase assays. Furthermore, we predicted arylacetamide deacetylase (AADAC) as a target of miR-1178–3p and examined its expression in ESCC tissues using Western blot. Lastly, we performed AADAC silencing and overexpression in Eca109 cells to study their impact on cellular phenotypic features, apoptosis, and their interaction with miR-1178–3p mimics and inhibitors.

The low expression of hsa_circ_0043,603 in ESCC tissue was associated with poor prognosis. Overexpression of hsa_circ_0043,603 inhibited ESCC growth, invasion, migration, and proliferation, while promoting apoptosis in vitro and suppressing tumor growth in vivo. hsa_circ_0043,603 achieved these effects by targeting the oncogenic miR-1178–3p. Furthermore, AADAC was identified as a target of miR-1178–3p, and its reduced expression was confirmed in ESCC tissues. Overexpression of AADAC in Eca109 cells resulted in suppressed cell growth, proliferation, migration, and invasion by regulating miR-1178–3p.

hsa_circ_0043,603 acts as a sponge for miR-1178–3p, leading to the regulation of AADAC expression and inhibition of ESCC development. These results suggest the potential of hsa_circ_0043,603 as a therapeutic and diagnostic target for ESCC.

1. Introduction

Esophageal cancer (EC) is known for its high malignancy and low 5-year survival rate, making it the eighth most common

malignant tumor worldwide [1]. In 2022, it is projected that there will be approximately 20,640 newly diagnosed cases of esophageal cancer in the United States, resulting in 16,410 deaths [2]. Esophageal cancer encompasses two primary histologic subtypes, namely esophageal squamous cell carcinoma (ESCC) and esophageal adenocarcinoma (EAC), which collectively account for the majority of cases. ESCC is prevalent in Eastern regions, whereas EAC is the predominant subtype observed in Western populations [3]. Esophageal carcinoma, particularly the squamous cell histology, has historically exhibited a significantly higher incidence in certain regions of Asia, including central Asia, northern China, and Iran. In rural China, EC has the highest incidence rate among all malignant tumors, with approximately half of the global cases diagnosed in China each year, primarily as ESCC [4]. Importantly, ESCC primarily manifests in the upper and middle regions of the esophagus and is closely linked to smoking and alcohol consumption. However, the specific risk factors for ESCC in non-Western populations are not as well-established [5]. Despite significant advancements in treatment techniques such as surgery and adjuvant radiotherapy and chemotherapy, the overall survival rate for EC remains low [6]. The majority of patients with esophageal squamous cell carcinoma (ESCC) are typically diagnosed at an advanced stage, which limits the feasibility of radical resection as a treatment option [7]. However, studies have demonstrated that early diagnosis and treatment can significantly enhance the prognosis of ESCC [8]. Hence, there is a pressing need to identify reliable tumor biomarkers that can facilitate the early detection of ESCC.

Circular RNA (circRNA) is a type of non-coding RNA characterized by its covalently closed loop structure. It exhibits notable features including stability, high expression abundance, species conservation, and cell/tissue specificity [9,10]. CircRNA is widely present in the human body and may act as an oncogene or tumor suppressor depending on the context [10–14]. circPLEKHM3 acts as a tumor suppressor in ovarian cancer cells by targeting the miR-9/AKT1 axis [15]. Similarly, circular RNA itchy E3 ubiquitin protein ligase (circ-ITCH) is a newly identified circular RNA that shows decreased expression levels in malignant tumors, including melanoma and ovarian cancer [16].

In ESCC, circRNA plays a crucial role in inhibition or development and progression of disease through their ability to function as miRNA sponges [17–20]. For instance, CircBCAR3 promotes the development and spread of esophageal cancer by sequestering miR-27a-3p [21]. Circ_0001686 enhances the advancement and radio resistance of esophageal cancer cells by modulating SPIN1 expression through the targeting of miR-876–5p [22]. circ-LRP6 promotes Myc-driven tumorigenesis, while hsa_circRNA6448-14 contributes to carcinogenesis in ESCC [23,24]. Additionally, several circRNAs have emerged as important prognostic factors in ESCC, including Circ-SLC7A5, circPVT1, and Circular FAT1 [25–28]. In contrast, circular RNA circTRPS1-2 functions by reducing ribosome production, thereby inhibiting the proliferation and migration of esophageal squamous cell carcinoma [29]. Another circ-RNA, circFAM120B functions as a tumor suppressor in ESCC through the miR-661/p38 MAPK pathway highlighting its potential as a therapeutic target in ESCC [30]. These findings suggest that circRNAs hold promise as valuable factors for the diagnosis, treatment, and prognosis of esophageal squamous cell carcinoma (ESCC). A recent study by Fan et al. identified the presence of hsa_circ_0043,603 and hsa_circ_0001946 in ESCC plasma samples and exosomes. Overexpression of hsa_circ_0001946 was found to significantly inhibit the growth of human esophageal carcinoma cells [31]. However, the regulatory effect of hsa_circ_0043,603 on ESCC remains unexplored, which serves as the research objective of our study.

2. Materials and methods

2.1. Clinical sample collection

A total of 30 ESCC tissues and their corresponding adjacent healthy tissues were collected from Xinxiang Central Hospital. The study procedures were conducted in accordance with the ethical standards outlined in the Helsinki Declaration and were approved by the Ethical Committee of Xinxiang Central Hospital (Clinical trial registration number: 2021–058). Informed consent was obtained from all patients participating in the study.

2.2. Cell culture, transfection, and treatment

The ESCC cell lines were cultured in RPMI 1640 medium (GIBCO BRL, USA) supplemented with 10% fetal bovine serum at 37 °C in a 5% CO2 environment. Transfection of circRNA plasmids, miRNA, and arylacetamide deacetylase (AADAC) plasmids was performed using Lipofectamine 2000 transfection reagent according to the manufacturer's instructions (Invitrogen, United States). For RNase R treatment, 2 µg of RNA extracted from cells was incubated with or without 3 µg of RNase R for 20 min at 37 °C, followed by purification. Additionally, 2 µg of RNA was treated with 1 µg of actinomycin D (Sigma) and assessed at 6, 12, and 18 h.

2.3. Nucleus-cytoplasm fractionation

Approximately 1×10^6 Eca109 cells were washed twice with pre-cooled PBS and centrifuged at 500 g for 5 min at 4 °C. RNA isolation was performed using the PARIS KIT50 RXNS Kit (life, AM1921) according to the manufacturer's protocols. The expression of hsa_circ_0043,603 was analyzed by qRT-PCR.

2.4. Fluorescence in situ hybridization (FISH)

For the FISH assay, a Cy3-labeled probe was employed. The samples were incubated with the probes in a buffer at room temperature for 3 h. The nuclei were labeled with 4,6-diamidino-2-phenylindole (DAPI) for 5 min. Images were captured using a
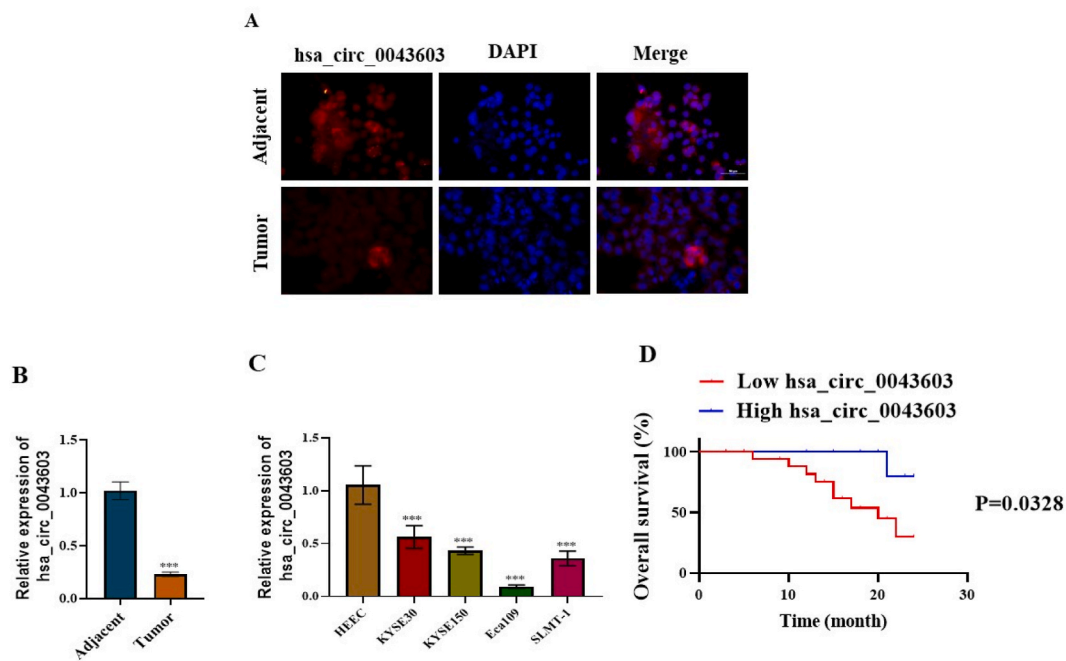
Fig. 1. Expression of hsa_circ_0043,603 in ESCC Tissues and Cell Lines. (A–B) The expression of hsa_circ_0043,603 in ESCC tissues and ESCC cell lines (KYSE30, KYSE 150, Eca 109, SLMT-1) was detected using FISH assay and qRT-PCR analysis (***p < 0.001). (C) qRT-PCR analysis revealed a remarkable suppression of hsa_circ_0043,603 expression in ESCC cell lines compared to the normal cell line HECC (***p < 0.001). (D) Kaplan-Meier curves showed the overall survival outcome of ESCC patients with high or low levels of hsa_circ_0043,603. Data are presented as mean ± standard deviation (SD). Statistical significance was determined using the *t*-test.

fluorescence microscope.

2.5. qRT-PCR

Total RNA, isolated using an RNA isolation kit, was reverse-transcribed into complementary DNA following the manufacturer's instructions. qRT-PCR was conducted using the ABI PRISM 7500 Sequence Detection System and SYBR-Green Premix Ex Taq from Takara Bio (Nojihigashi, Kusatsu, Japan). U6 and Glyceraldehyde-3-phosphate dehydrogenase (GAPDH) served as internal controls. The gene expression was analyzed using the $2^{-\Delta\Delta CT}$ method.

2.6. Western blot

Proteins were extracted from ESCC cells/tissues using RIPA lysis buffer from Thermo Scientific (USA). Protein quantification was performed using a BCA kit. Thirty μg of protein were loaded onto an SDS-PAGE gel and separated. The proteins were then transferred to a PVDF membrane and blocked with nonfat milk at 37 °C for 1 h. Next, primary antibodies against AADAC and GAPDH were added and incubated overnight at 4 °C. Subsequently, the membrane was incubated with an HRP-conjugated secondary antibody for 1 h at 37 °C. Finally, chemiluminescence and a gel imager were used to analyze the results.

2.7. Cell counting Kit-8 (CCK-8) assay

Eca109 cells were seeded in 96-well plates at a density of 4×10^3 cells per well. Then, 10 μl of CCK-8 solution was added to each well, and the cells were observed at 0, 24, 48, and 72 h. The optical density at 450 nm was measured using a microplate reader, following the instructions provided by the manufacturer.

2.8. 5-Ethynyl-20-Deoxyuridine (EdU) assay

Eca109 cells were seeded in 96-well plates and treated with polylysine for 4 h at 37 °C. After that, the cells were dried, fixed, and stained. The resulting images were captured using laser confocal microscopy after incubating the cells with EdU for 24–48 h and subsequent fixation.
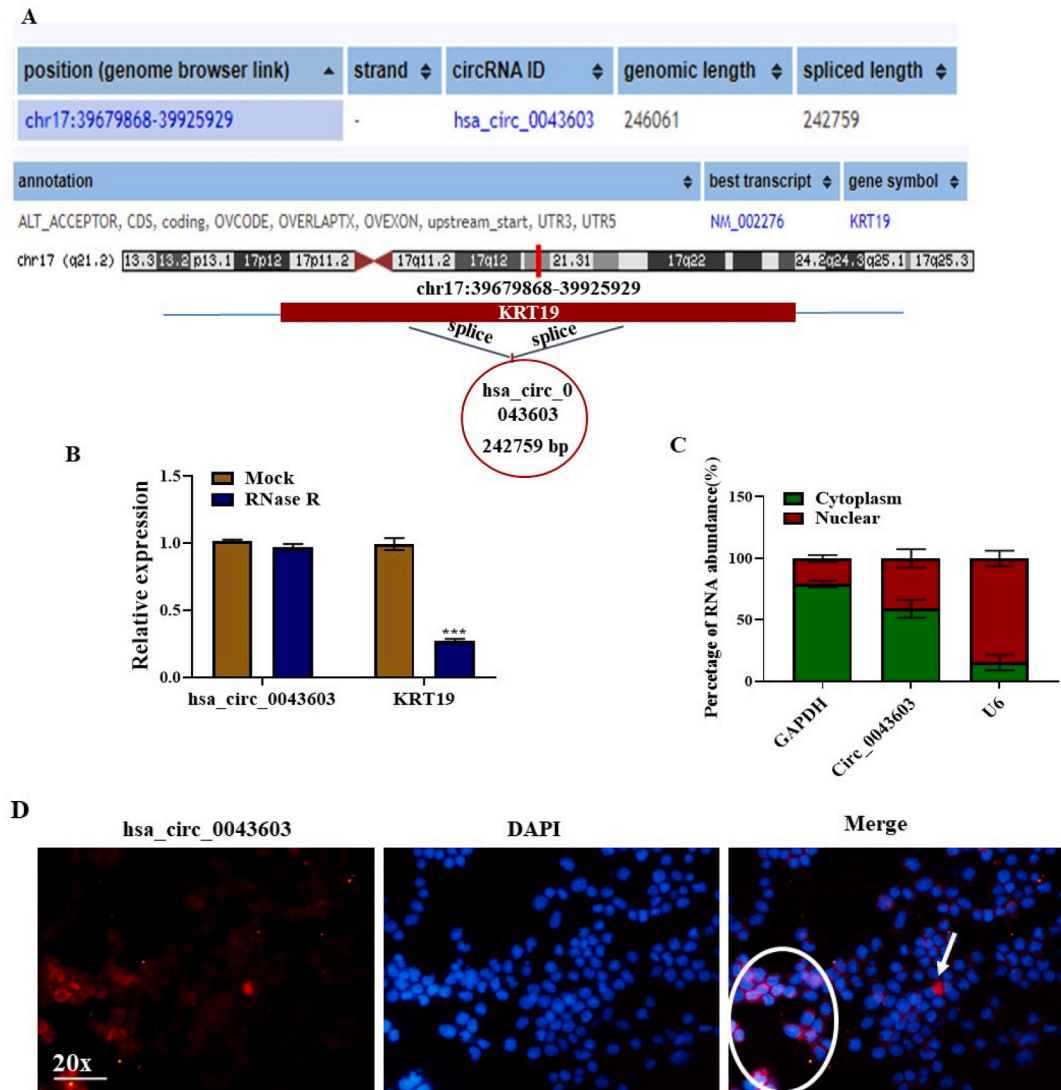
Fig. 2. Characteristics of hsa_circ_0043,603 in ESCC. (A) Analysis of circBase database indicates that KRT19 is the primary transcript of hsa_-circ_0043,603 located on chromosome 17. **(B)** qRT-PCR analysis of linear KRT19 mRNA and hsa_circ_0043,603 in Eca109 cells treated with RNase R. *** indicates $p < 0.001$ compared to mock. **(C)** RNA nuclear-cytoplasmic localization analysis and **(D)** FISH assay to determine the subcellular localization of hsa_circ_0043,603 in Eca109 cells.

2.9. Transwell invasion assay

The transwell chambers with 8-μm-pore Millipore membranes were filled with growth factor reduced Matrigel (1 mg/ml, Corning). The upper chambers were coated with 500 μl of serum-free medium containing 2×104 Eca109 cells, while the lower chambers were coated with 1 ml of complete medium. The chambers were then incubated at 37 °C for 24 h. The invaded cells were fixed and stained with Giemsa (HiMedia Labs). Image capturing was performed using an inverted microscope (CX41, Olympus), and ImageJ software was utilized for analysis.

2.10. Cell migration assay

Eca109 cells were cultured in six-well plates. A straight scratch was made on the cell monolayer using pipette tips. Images of the scratched area were captured at 0 h and 24 h. The relative migration rate was calculated as follows: (initial width - width at 24 h)/ initial width $\times$ 100%.

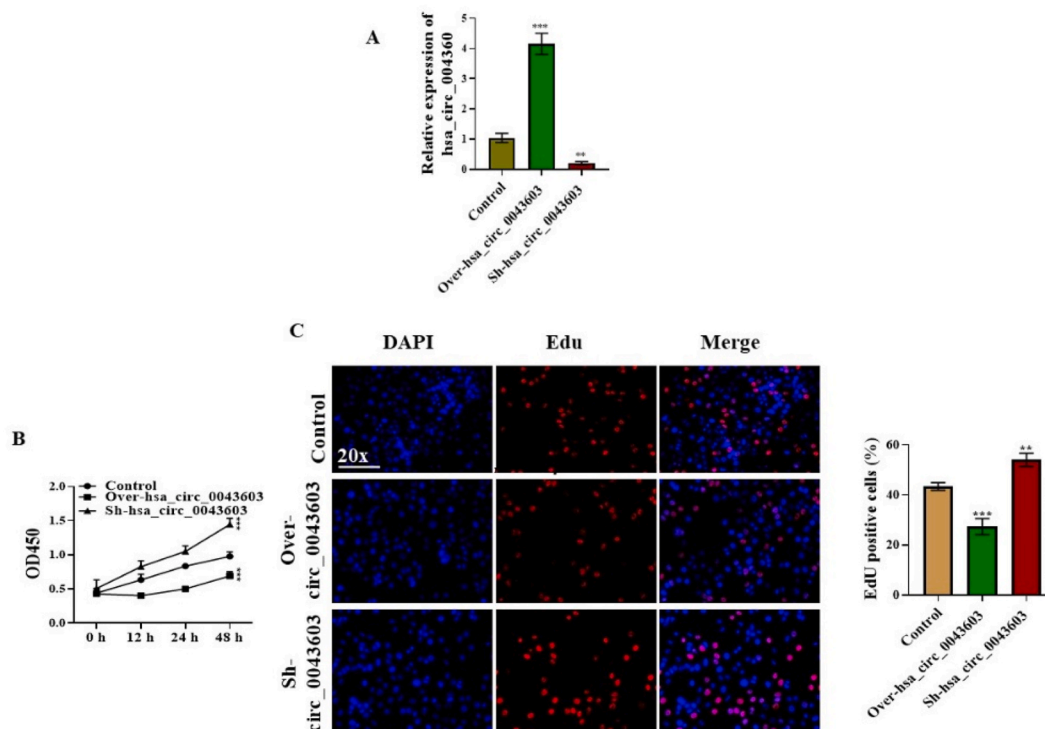**Fig. 3. Functional impact of hsa_circ_0043,603 on cell characteristics in Eca109 cells**. **(A)** Expression of hsa_circ_0043,603 in Eca109 cells detected by qRT-PCR. **(B, C)** Cell proliferation assessed by CCK-8 analysis and Edu assay. **(D, E)** Cell invasion and migration analyzed by transwell and migration assays. **(F)** Apoptosis evaluated by flow cytometry. **, $p < 0.01$, ***, $p < 0.001$, Vs control.

2.11. Flow cytometry analysis

Eca109 cells were seeded in six-well plates at a density of 5×105 cells per well. The cells were cultured for 48 h at 37 °C. Afterward, the cells were stained using the Annexin V-FITC/PI apoptosis detection kit (BD Biosciences). The results were analyzed using a FACSCalibur flow cytometer (BD Biosciences, San Jose, CA, USA).

2.12. Luciferase reporter assay

The mutant and wild-type circ0120816 and AADAC sequences were synthesized and inserted into the pmiR-GLO reporter vector (Promega). These vectors, along with miR-1178–3p mimics, were transfected into Eca109 cells. The cells were then incubated for 48 h. The Dual-GLO® Luciferase Assay System Kit (Promega, USA) and a Fluorescence/Multi-Detection Microplate Reader (BioTek, USA) were used for analysis.

2.13. RNA immunoprecipitation (RIP) assay

The Magna RIP RNA-Binding Protein Immunoprecipitation Kit (Millipore, USA) was utilized to perform the RIP assay and investigate the relationship between hsa_circ_0043,603, AADAC, and miR-1178–3p. A total of 1×106 Eca109 cells were lysed using RIP lysis buffer. Magnetic beads conjugated with IgG or antibodies against Ago2 were then added and incubated at 4 °C for 12 h. Proteinase K was subsequently introduced and incubated at 37 °C for 30 min. The IP RNAs were isolated by washing twice with RIP buffer.

2.14. Tumor xenograft mice model

Nude BALB/c mice (6 weeks old) were housed in a pathogen-free facility under a 12-h light/dark cycle. After one week, the mice were randomly divided into three groups, each consisting of five mice. The mice were then injected with either Eca109 cells (1×10^{6}) transfected with Over-circ_0043,603 or sh-circ_0043,603 or a negative control (NC, blank control Eca109 cells) based on their group assignment. After four weeks, the mice were euthanized, and tumor tissues were collected and measured. All animal experimental procedures were conducted in accordance with the guidelines approved by the Animal Welfare and Research Ethics Committee of Xinxiang Central Hospital.
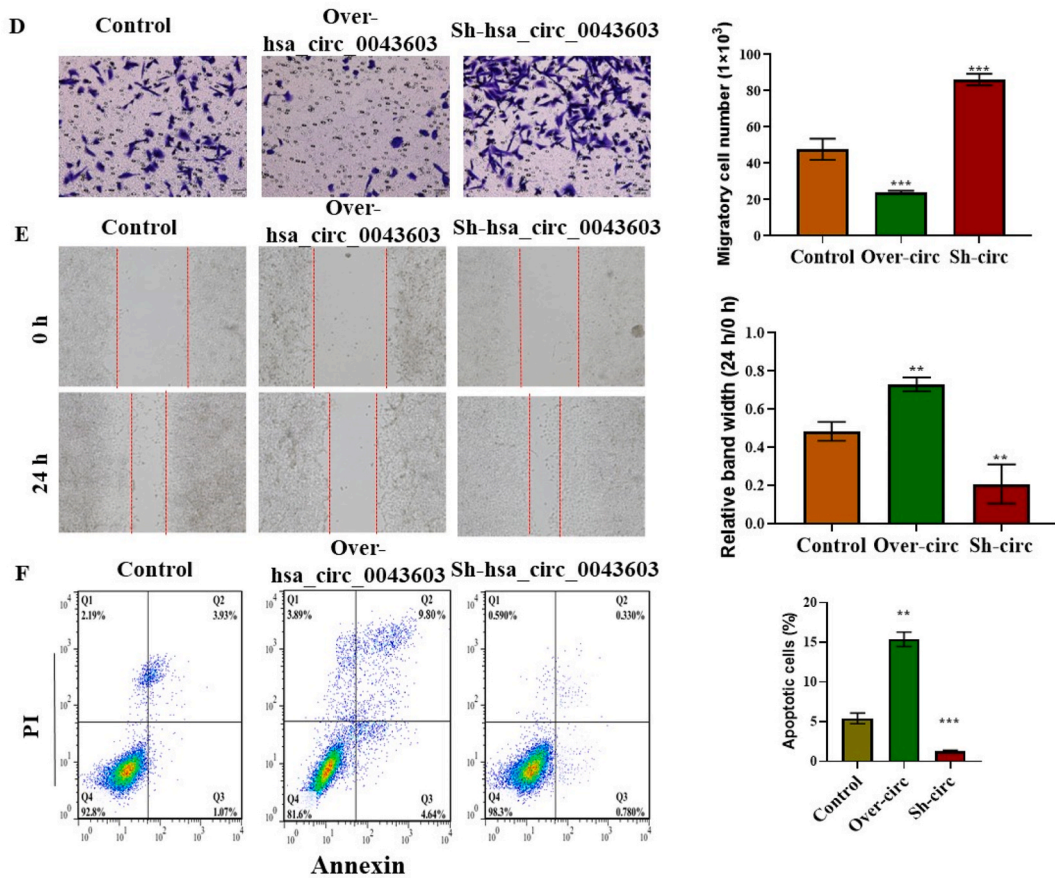
Fig. 3. (*continued*).

2.15. Ki-67 immunohistochemical staining

The ESCC tumor tissues were embedded in paraffin and cut into 4-μm sections. Subsequently, the sections were deparaffinized, rehydrated, and treated with 3% hydrogen peroxide for 10 min. The primary antibody against Ki67 (Santa Cruz, CA, USA) was applied at room temperature and incubated for 1 h. Following that, an HRP-labeled secondary antibody was added and incubated for 30 min at 37 °C. Staining was performed using 3,3-diaminobenzidine (DAB) and hematoxylin. The images were captured using a microscope.

2.16. Statistical analysis

Statistical analysis was conducted using SPSS 21.0 software (IBM, Chicago, USA). The data were presented as mean ± standard deviation (SD). The *t*-test and ANOVA were used to assess differences between two or more than two groups, respectively. Pearson's chi-square test was employed for correlation analysis. A p value of $*p < 0.05$, $**p < 0.01$, $***p < 0.001$ were considered statistically significant.

3. Results

3.1. Downregulation of hsa_circ_0043,603 in ESCC tissue

The expression of hsa_circ_0043,603 was found to be significantly lower in ESCC tissues compared to adjacent tissues (Fig. 1A and B). Similarly, the expression of hsa_circ_0043,603 was remarkably suppressed in ESCC cell lines compared to the normal cell line HECC (Fig. 1C). Moreover, the survival analysis showed that ESCC patients with low level of hsa_circ_0043,603 had worse prognosis relative to those with high hsa_circ_0043,603 expression (P = 0.0328). These findings suggest that hsa_circ_0043,603 acts as a tumor suppressor and its expression is reduced during the progression of ESCC.

Fig. 4. Molecular interaction between hsa_circ_0043,603 and miR-1178-3p. (A) Predicted binding sites of hsa_circ_0043,603 with miR-1178–3p based on Starbase 2.0. **(B,C)** Expression levels of miR-1178–3p in ESCC tissues measured by FISH and qRT-PCR. **(D)** Dual luciferase reporter assay demo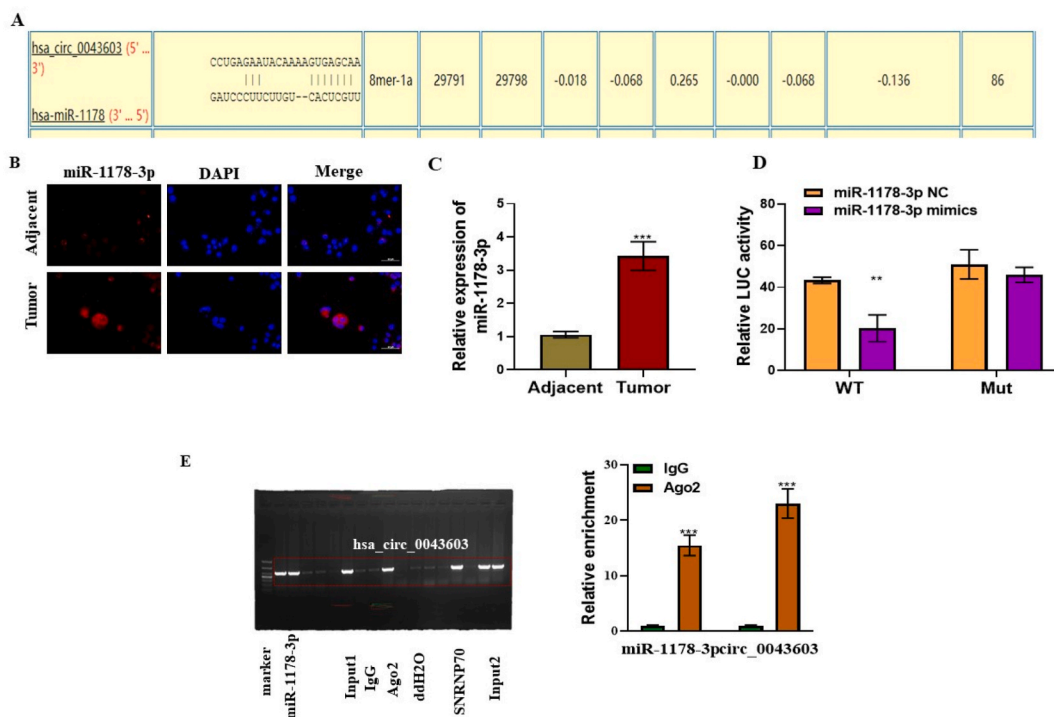nstrating the binding between miR-1178–3p and hsa_circ_0043,603. **(E)** RIP assay showing the binding between miR-1178-3p and hsa_circ_0043,603. **p < 0.01, ***p < 0.001.

3.2. Characteristics of hsa_circ_0043,603 in ESCC

The circBase database analysis revealed that hsa_circ_0043,603 originates from the KRT19 transcript located on chromosome 17 (Fig. 2A). qRT-PCR analysis demonstrated that the linear KRT19 mRNA in Eca109 cells was significantly degraded after 20 min of RNase R treatment, while there was no significant difference in hsa_circ_0043,603 expression (Fig. 2B). These findings suggest that hsa_circ_0043,603 is more stable in ESCC cells compared to linear KRT19 mRNA. Additionally, RNA nuclear-cytoplasmic localization and fluorescence in situ hybridization (FISH) assay indicated that hsa_circ_0043,603 predominantly localizes in the cytoplasm of Eca109 cells, with minimal presence in the nucleus (Fig. 2C and white arrow and circle in 2D).

3.3. Overexpression of hsa_circ_0043,603 inhibited cell proliferation, migration, invasion while promoted apoptosis

To investigate the functional impact of hsa_circ_0043,603 on cellular phenotypic characteristics, we manipulated its expression in Eca109 cells using overexpression and silencing plasmids. Successful transfection of hsa_circ_0043,603 overexpression (over-hsa_circ_0043,603) and hsa_circ_0043,603 silencing (sh-hsa_circ_0043,603) in the Eca109 cells is shown (Fig. 3A). CCK-8 analysis revealed that overexpression of hsa_circ_0043,603 significantly suppressed Eca109 cell proliferation, while silencing hsa_circ_0043,603 had the opposite effect (Fig. 3B). Similarly, Edu staining demonstrated that overexpressing hsa_circ_0043,603 led to reduced cell proliferation, whereas knockdown of hsa_circ_0043,603 had the opposite effect (Fig. 3C). Transwell assay revealed that overexpression of hsa_circ_0043,603 markedly inhibited the migration ability of Eca109 cells (Over-circ group), while silencing hsa_circ_0043,603 enhanced cell migration (sh-circ group), as depicted in Fig. 3D. Furthermore, the cell migration assay at 24 h indicated that overexpression of hsa_circ_0043,603 decreased cell migration (Over-circ group), while silencing hsa_circ_0043,603 promoted cell migration (Fig. 3E). Lastly, flow cytometry analysis revealed a significant increase in apoptosis rate in cells overexpressing hsa_circ_0043,603 and a decrease in apoptosis rate in cells with suppressed hsa_circ_0043,603 (Fig. 3F).

3.4. hsa_circ_0043,603 is a molecular sponge of mir-1178–3p

To predict the miRNA sponge of hsa_circ_0043,603, Starbase 2.0 was utilized, and miR-1178–3p was identified as a potential target of hsa_circ_0043,603 as hsa_circ_0043,603 sequences with binding sites to miR-1178–3p (Fig. 4A). Subsequently, the expression of miR-1178–3p in ESCC tissues was evaluated using FISH and PCR that revealed higher levels in ESCC tissues compared to adjacent tissues (Fig. 4B and C). The relative luciferase activity analysis showed a significant decrease in luciferase activity in wild-type cells
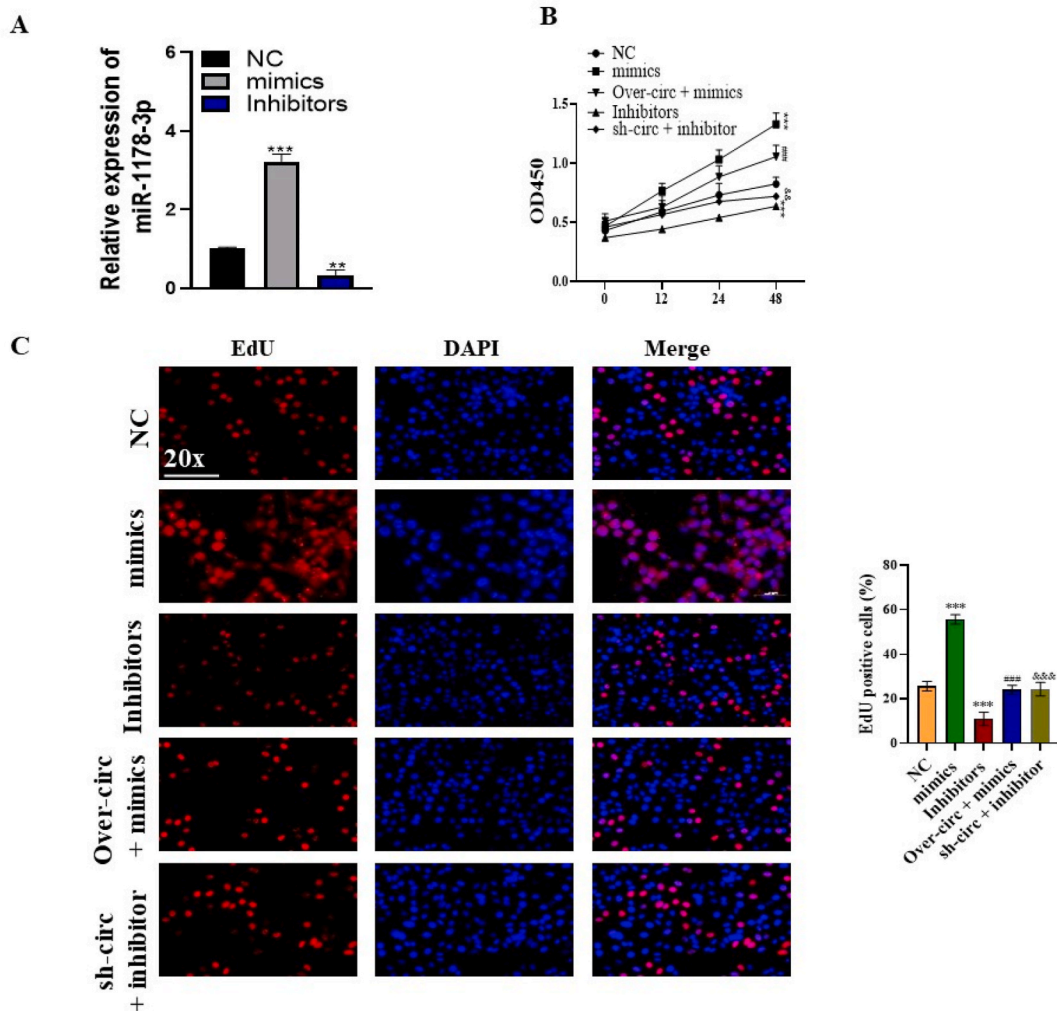
Fig. 5. Functional effects of miR-1178-3p on cell proliferation, migration, invasion, and apoptosis regulated by hsa_circ_0043,603. (A) qRT-PCR analysis of miR-1178–3p expression in transfected Eca109 cells. **(B)** CCK-8 analysis and **(C)** Edu assays to assess cell proliferation in Eca109 cells transfected with different vectors i.e., control, miR-1178–3p mimics, miR-1178–3p inhibitor, Eca109 cells overexpressing circ_0043,603 and miR-1178–3p mimics, and Eca109 cells overexpressing circ_0043,603 and miR-1178–3p inhibitor. **(D–F)** Transwell and cell migration assays used to evaluate the invasion and migration ability of Eca109 cells transfected with miR-1178–3p and hsa_circ_0043,603. **(G)** Assessment of apoptosis in Eca109 cells transfected with different vectors. *, $p < 0.05$, **, $p < 0.01$, ***, $p < 0.001$; #, $p < 0.05$, ###, $p < 0.001$; &, $p < 0.05$, &&&, $p < 0.001$.

transfected with miR-1178–3p mimic, while no change was observed in mutant cells transfected with either miR-1178–3p mimic or control (Fig. 4D). Additionally, RIP experiments demonstrated higher expression of hsa_circ_0043,603 and miR-1178–3p in the Ago2 group compared to the IgG group (Fig. 4E). Collectively, these findings indicate an interaction and binding between hsa_circ_0043,603 and miR-1178–3p, suggesting that hsa_circ_0043,603 acts as a sponge for miR-1178–3p in ESCC cells.

3.5. miR-1178–3p promotes cell proliferation, migration, and invasion while inhibiting apoptosis via interaction with hsa_circ_0043,603

As shown in Fig. 5A, the expression of miR-1178–3p was significantly increased or decreased with transfection of corresponding mimics or inhibitors. CCK-8 analysis demonstrated that Eca109 cell proliferation was promoted by miR-1178–3p mimics and suppressed by miR-1178–3p inhibitors (Fig. 5B). Edu assay indicated that miR-1178–3p mimics increased the Edu positive cells and miR-1178–3p inhibitors showed the opposite (Fig. 5C). Transwell assay indicated that miR-1178–3p mimics enhanced the invasion ability of Eca109 and miR-1178–3p inhibitors showed the opposite (Fig. 5D). Cell migration assay indicated that miR-1178–3p mimics increased the Eca109 cell migration and miR-1178–3p inhibitors showed the opposite (Fig. 5E and F). The apoptosis rate was significantly inhibited by overexpressed miR-1178–3p and promoted by suppressed miR-1178–3p (Fig. 5G). In all these experiment,
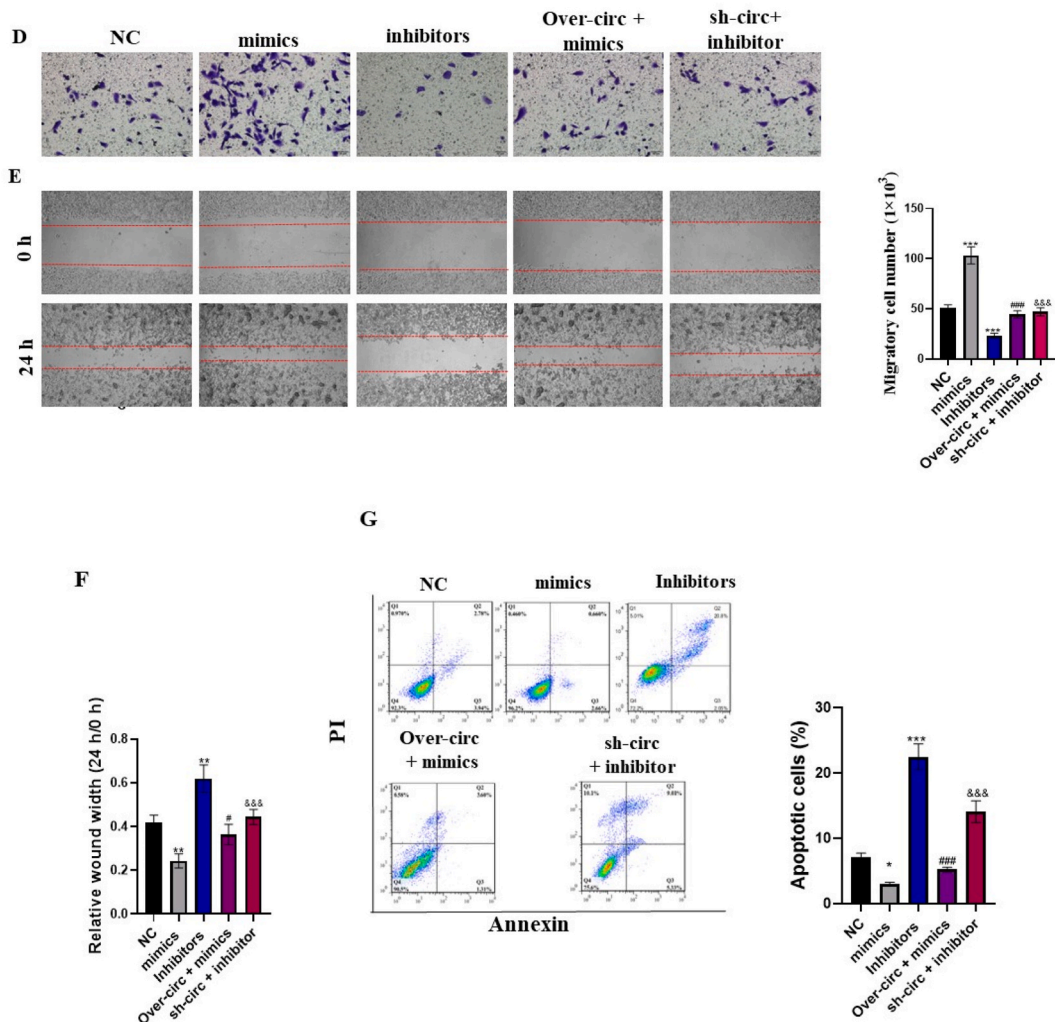
Fig. 5. (*continued*).

overexpression of hsa_circ_0043,603 reversed the regulation of ESCC progression by miR-1178–3p (Fig. 5B–G). Overall, miR-1178–3p promotes cell proliferation, migration, and invasion while inhibiting apoptosis, and its effects are reversed by hsa_circ_0043,603 in ESCC.

3.6. AADAC is a target of mir-1178–3p

TargetScan analysis predicted that miR-1178–3p targets AADAC with a binding site at position 301–308 of the 3′ UTR (Fig. 6A). We investigated the expression of AADAC in ESCC tissues using Western blot assay that revealed significantly lower expression of AADAC in ESCC tissues compared to adjacent control tissues (Fig. 6B). In agreement, luciferase activity was significantly decreased in the wild-type group but not in the mutant-type group (Fig. 6C). Moreover, RIP experimental results demonstrated increased expression of AADAC in the Ago2 group compared to the IgG group (Fig. 6D). These findings confirm that AADAC is targeted by miR-1178–3p.

3.7. AADAC overexpression inhibits cell phenotypic features and promotes apoptosis via mir-1178–3p regulation

We investigated the impact of AADAC on cellular phenotypic features. AADAC expression was manipulated in Eca109 cells using Over-AADAC or Sh-AADAC plasmids, as shown in Fig. 7A. The results revealed that Over-AADAC led to decreased cell proliferation, as indicated by a decrease in Edu-positive cells, while suppression of AADAC increased proliferation (Fig. 7B). Transwell assay demonstrated that Over-AADAC inhibited the migratory ability of Eca109 cells, whereas the sh-AADAC group showed enhanced migration (Fig. 7C). Cell migration assay further confirmed reduced migration in the Over-AADAC group and increased migration in the sh-AADAC group (Fig. 7D). Additionally, overexpressing AADAC significantly increased the apoptosis rate, while suppressing AADAC decreased it (Fig. 7E). Importantly, the effects of AADAC were partially reversed by miR-1178–3p, suggesting that

Fig. 6. miR-1178-3p targets AADAC. (A) TargetScan analysis predicted the binding site of miR-1178–3p with AADAC. **(B)** Western blot analysis revealed the expression of AADAC in ESCC tissues. **(C)** Dual luciferase reporter assay detected the binding of miR-1178–3p and AADAC, ***p < 0.001, miR-1178–3p mimics group vs NC group. **(D)** RIP assay detected the binding of miR-1178–3p and AADAC, ***p < 0.001, Ago2 group vs IgG group.

overexpressed AADAC suppresses cell growth, proliferation, migration, and invasion by regulating miR-1178–3p (Fig. 7B–E).

3.8. Overexpression hsa_circ_0043,603 inhibited the tumor growth of ESCC in vivo

Xenograft tumor models were established by injecting Eca109 cells overexpressing or silenced for circ_0043,603 into mice. The results demonstrated that overexpression of hsa_circ_0043,603 led to a reduction in tumor size, while suppression of hsa_circ_0043,603 increased tumor size (Fig. 8A). Ki-67 and TUNEL assays revealed a significant inhibition of proliferation and a notable increase in apoptosis in the hsa_circ_0043,603 overexpression group compared to the NC group (Fig. 8B and C). Xenografts generated by injecting Eca109 cells with silenced hsa_circ_0043,603 exhibited increased proliferation and decreased apoptosis, contrasting with the effects observed in xenografts with hsa_circ_0043,603 overexpression. (Fig. 8B and C). These findings indicate that hsa_circ_0043,603 functions as a tumor suppressor, inhibiting tumor growth in vivo.

4. Discussion

ESCC, the main pathological type of esophageal cancer, has a high mortality rate despite advancements in surgical, radio-therapeutic, and chemotherapeutic approaches [7,17]. Therefore, identifying effective treatment strategies is urgently needed. In this study, we discovered that hsa_circ_0043,603 was downregulated in ESCC tissues. Moreover, we found that hsa_circ_0043,603 acted as a tumor suppressor by regulating AADAC expression through its interaction with miR-1178–3p. These findings suggest that hsa_-circ_0043,603 holds promise as a therapeutic target for ESCC patients.

CircRNAs are a recently discovered class of non-coding RNAs with unique structures. They are widely present in eukaryotes, mainly in the cytoplasm [32]. Increasing evidence indicates that circRNAs play diverse regulatory roles in cancer progression, including ESCC. For instance, Circ-DLG1 and Circ-TTC17 were shown to promote ESCC proliferation and progression, respectively [33,34]. Further-more, certain circRNAs have been identified as prognostic markers in ESCC. For instance, Wang et al. identified four circRNAs that serve as prognostic markers in ESCC through RNA sequencing of circRNA [35]. Additionally, Takaki et al. demonstrated that Circular FAT1 acts as a prognostic factor and suppresses ESCC progression [28]. A previous study has demonstrated that hsa_circ_0043,603 is downregulated in ESCC tumor tissues, suggesting its potential as a diagnostic biomarker for ESCC. The study reported an AUC (Area under the curve) value of 0.836 and 92% specificity [36]. However, the investigation into the role of hsa_circ_0043,603 in other cancers remains limited or scarce. In this study, we confirmed that hsa_circ_0043,603 was downregulated in ESCC tissues and that its overexpression inhibited invasion, migration, and proliferation while promoting apoptosis in ESCC cells. Furthermore, xenograft experiments demonstrated that hsa_circ_0043,603 suppressed tumor growth and volume, reduced proliferation and promoted apoptosis, underscoring its role as a tumor suppressor in ESCC progression.

Recent studies have revealed that circRNAs can regulate gene expression by acting as molecular sponges for miRNAs, thereby sequestering them, and preventing their inhibition of target genes [37,38]. In ESCC, circRNA-miRNA ceRNA networks have been shown to play crucial roles in cancer progression. For example, circRNA_141,539 functions as an oncogenic factor through the miR-4469/CDK3 axis, while circLPAR3 facilitates ESCC progression via the HMGB1/miR-375/miR-433 axis [39,40]. Additionally, circAGFG1 is sponged by miR-4306, thus stimulating ESCC progression by regulating MAPRE2 [41]. In our study, we demonstrated the presence of binding sites between hsa_circ_0043,603 and miR-1178–3p, as well as between AADAC and miR-1178–3p. Previous research has associated miR-1178–3p with the promotion of invasion, migration, and proliferation in nasopharyngeal carcinoma by

(caption on next page)

Fig. 7. Effects of AADAC Overexpression on Cell Phenotypic Features and Apoptosis Regulated by miR-1178-3p. (A) AADAC expression in Eca109 cells detected by qRT-PCR. **(B)** Proliferation of Eca109 cells treated with different vectors assessed by EdU assay. **(C, D)** Invasion and migration ability of Eca109 cells regulated by AADAC and miR-1178–3p, evaluated using Transwell and cell migration assay. **(E)** Apoptosis regulated by AADAC and miR-1178–3p, analyzed by flow cytometry. Statistical significance is denoted as follows: *, $p < 0.05$; **, $p < 0.01$; ***, $p < 0.001$. ##, $p < 0.05$; ###, $p < 0.001$. &, $p < 0.05$; &&&, $p < 0.001$.
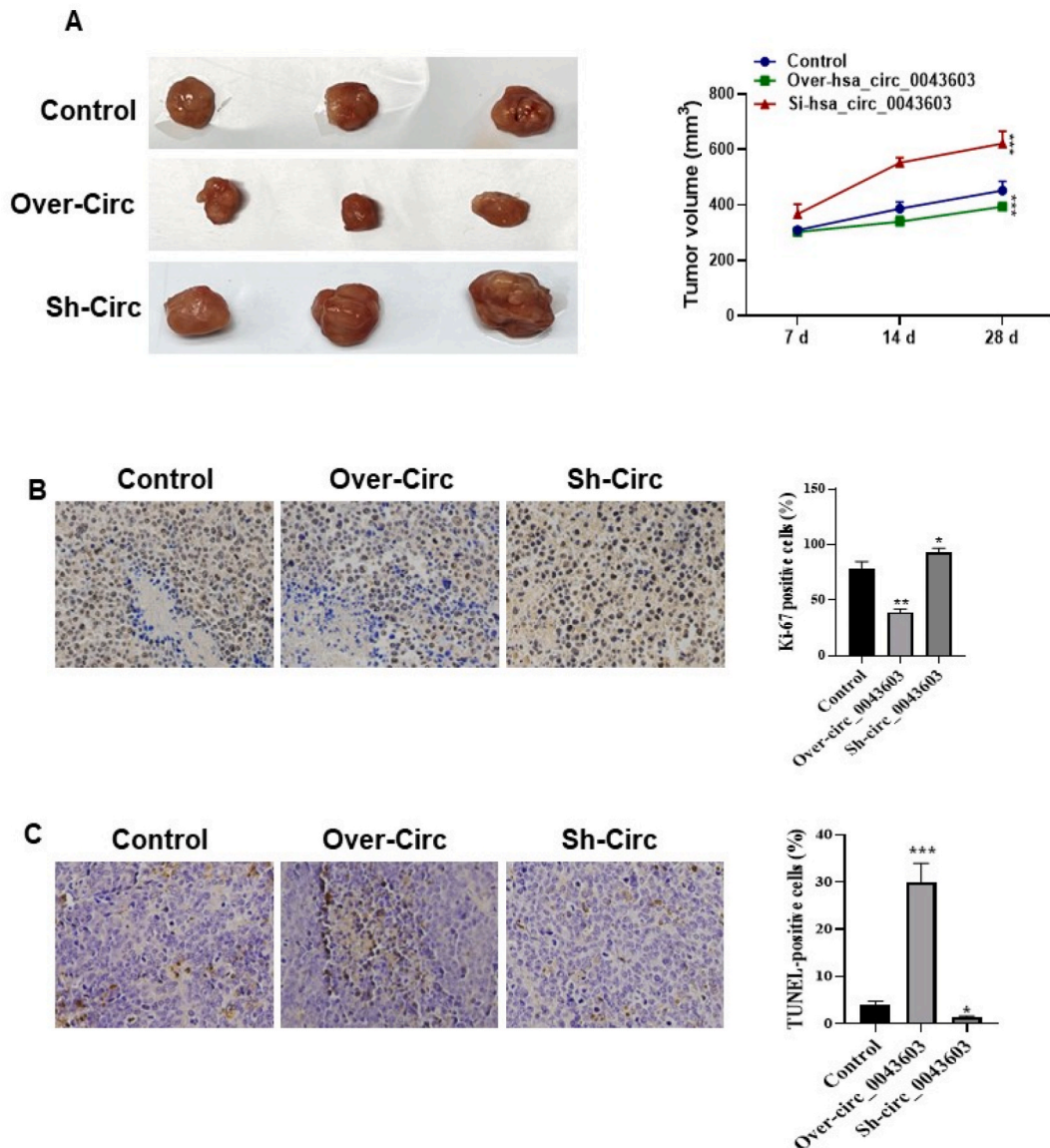
Fig. 8. Tumor Growth Inhibition by hsa_circ_0043,603 Overexpression in ESCC In Vivo. (A) Tumor size in xenografts injected with cells silenced or expressed for hsa_circ_0043,603. **(B & C)** Proliferation and apoptosis data of xenografts assessed using Ki-67 and TUNEL assays. Statistical significance is denoted as *, $p < 0.05$; ***, $p < 0.001$.

targeting STK4 and bladder cancer by regulating p21 [42,43]. Interestingly, miR-1178–3p has anti-tumor effects in papillary thyroid cancer, inhibiting proliferation, apoptosis, migration, invasion, and angiogenesis of cancer cells by targeting YWHAH [44]. However, its biological roles in the progression of ESCC are rarely reported. Our findings revealed that miR-1178–3p promotes cell invasion, migration, and proliferation and is sponged by hsa_circ_0043,603. AADAC was directly targeted by miR-1178–3p. Several studies have highlighted the significant roles of AADAC in cancer. For instance, Liu et al. conducted integrated bioinformatics analysis and identified nine hub genes, including AADAC, that are associated with the pathogenesis and prognosis of gastric cancer [45]. Similarly, Wu et al. developed a nine-gene signature, which includes AADAC, for predicting the prognosis of gastric cancer [46]. A study has shown that AADAC plays a protective role in metastatic colorectal cancer cells by preventing lipid peroxidation-induced ferroptosis in an

SLC7A11-dependent manner [47]. Additionally, another study has demonstrated that AADAC can serve as both a prognostic biomarker and a therapeutic target in ESCC [48]. Based on the analysis of the TCGA database, AADAC was found to be downregulated in esophageal adenocarcinoma [49]. Our experimental data revealed that overexpression of AADAC restored the promoting effects of miR-1178–3p on ESCC cell migration, invasion, and proliferation. This suggests that miR-1178–3p promotes malignant behaviors of ESCC cells by negatively regulating AADAC expression. Overall, our findings indicate that hsa_circ_0043,603 regulates AADAC expression in ESCC through its interaction with miR-1178–3p.

This study also had several limitations. Firstly, the biological functions of hsa_circ_0043,603 were only investigated in Eca109 cells, and the experiments were not validated using other ESCC cell lines. Secondly, the impact of AADAC on ESCC tumor growth in vivo was not examined. Thirdly, the effects of AADAC overexpression on the enhanced enhancement of ESCC cells induced by hsa_circ_0043,603 silencing were not presented. These limitations will be addressed in our future research.

5. Conclusion

Our study provides compelling evidence that hsa_circ_0043,603 is downregulated in ESCC tissues and is associated with a poor prognosis. Mechanistically, we have demonstrated that hsa_circ_0043,603 inhibits ESCC progression by regulating AADAC expression through the sponging of miR-1178–3p (Graphical abstract). Given the distinct expression pattern of hsa_circ_0043,603 in ESCC, it has the potential to serve as a tissue biopsy biomarker for ESCC patients. Moreover, circRNA-based anti-cancer agents or circRNA-targeted drugs, utilizing various delivery systems such as nanocarriers or engineered exosomes, may offer promising alternatives for future cancer therapies. These findings strongly suggest that hsa_circ_0043,603 holds promise as a diagnostic and therapeutic target for ESCC.

Ethics approval and consent to participate

The experiments were approved by the Ethics Committee of Xinxiang Central Hospital (Clinical trial registration number: 2021–058). The contents of this study are under full compliance with government policy and the Declaration of Helsinki.

Funding

Author contribution statement

Xuezhong Wang: Conceived and designed the experiments; Performed the experiments; Analyzed and interpreted the data; Contributed reagents, materials, analysis tools or data; Wrote the paper. Zhiguang Liu; Yalong Du; Shuguang Hao; Bing Zhao: Performed the experiments; Analyzed and interpreted the data; Wrote the paper.

Data availability statement

Data will be made available upon request.

Declaration of competing interest

None.

Appendix A. Supplementary data

Supplementary data to this article can be found online at https://doi.org/10.1016/j.heliyon.2023.e19807.

References

[1] F.L. Huang, S.J. Yu, Esophageal cancer: risk factors, genetic association, and treatment, Asian J. Surg. 41 (3) (2018) 210–215.
[2] R.L. Siegel, K.D. Miller, H.E. Fuchs, A. Jemal, Cancer statistics, 2022, CA A Cancer J. Clin. 72 (1) (2022) 7–33.
[3] M.B. Cook, W.H. Chow, S.S. Devesa, Oesophageal cancer incidence in the United States by race, sex, and histologic type, 1977-2005, Br. J. Cancer 101 (5) (2009) 855–859.
[4] D.J. Uhlenhopp, E.O. Then, T. Sunkara, V. Gaduputi, Epidemiology of esophageal cancer: update in global trends, etiology and risk factors, Clin J Gastroenterol 13 (6) (2020) 1010–1021.
[5] J. Lagergren, E. Smyth, D. Cunningham, P. Lagergren, Oesophageal cancer, Lancet (London, England) 390 (10110) (2017) 2383–2396.
[6] E. Bollschweiler, P. Plum, S.P. Monig, A.H. Holscher, Current and future treatment options for esophageal cancer in the elderly, Expet Opin. Pharmacother. 18 (10) (2017) 1001–1010.
[7] K. Harada, J.E. Rogers, M. Iwatsuki, K. Yamashita, H. Baba, J.A. Ajani, F1000Res, Recent advances in treating oesophageal cancer 9 (2020).
[8] Z.W. Reichenbach, M.G. Murray, R. Saxena, D. Farkas, E.G. Karassik, A. Klochkova, K. Patel, C. Tice, T.M. Hall, J. Gang, et al., Clinical and translational advances in esophageal squamous cell carcinoma, Adv. Cancer Res. 144 (2019) 95–135.

[9] L.S. Kristensen, M.S. Andersen, L.V.W. Stagsted, K.K. Ebbesen, T.B. Hansen, J. Kjems, The biogenesis, biology and characterization of circular RNAs, Nat. Rev. Genet. 20 (11) (2019) 675–691.

[10] H. Zhang, Y. Shen, Z. Li, Y. Ruan, T. Li, B. Xiao, W. Sun, The biogenesis and biological functions of circular RNAs and their molecular diagnostic values in cancers, J. Clin. Lab. Anal. 34 (1) (2020), e23049.

[11] S. Meng, H. Zhou, Z. Feng, Z. Xu, Y. Tang, P. Li, M. Wu, CircRNA: functions and properties of a novel potential biomarker for cancer, Mol. Cancer 16 (1) (2017) 94.

[12] K.Y. Hsiao, H.S. Sun, S.J. Tsai, Circular RNA - new member of noncoding RNA with novel functions, Exp. Biol. Med. 242 (11) (2017) 1136–1141.

[13] J. Fang, H. Hong, X. Xue, X. Zhu, L. Jiang, M. Qin, H. Liang, L. Gao, A novel circular RNA, circFAT1(e2), inhibits gastric cancer progression by targeting miR-548g in the cytoplasm and interacting with YBX1 in the nucleus, Cancer Lett. 442 (2019) 222–232.

[14] Z. Li, Y. Ruan, H. Zhang, Y. Shen, T. Li, B. Xiao, Tumor-suppressive circular RNAs: mechanisms underlying their suppression of tumor occurrence and use as therapeutic targets, Cancer Sci. 110 (12) (2019) 3630–3638.

[15] L. Zhang, Q. Zhou, Q. Qiu, L. Hou, M. Wu, J. Li, X. Li, B. Lu, X. Cheng, P. Liu, et al., CircPLEKHM3 acts as a tumor suppressor through regulation of the miR-9/BRCA1/DNAJB6/KLF4/AKT1 axis in ovarian cancer, Mol. Cancer 18 (1) (2019) 144.

[16] Y. Li, Y.Z. Ge, L. Xu, R. Jia, I.T.C.H. Circular Rna, A novel tumor suppressor in multiple cancers, Life Sci. 254 (2020), 117176.

[17] Q. Feng, H. Zhang, D. Yao, W.D. Chen, Y.D. Wang, Emerging role of non-coding RNAs in esophageal squamous cell carcinoma, Int. J. Mol. Sci. 21 (1) (2019).

[18] Y. Shi, N. Fang, Y. Li, Z. Guo, W. Jiang, Y. He, Z. Ma, Y. Chen, Circular RNA LPAR3 sponges microRNA-198 to facilitate esophageal cancer migration, invasion, and metastasis, Cancer Sci. 111 (8) (2020) 2824–2836.

[19] Y. Zhong, Y. Du, X. Yang, Y. Mo, C. Fan, F. Xiong, D. Ren, X. Ye, C. Li, Y. Wang, et al., Circular RNAs function as ceRNAs to regulate and control human cancer progression, Mol. Cancer 17 (1) (2018) 79.

[20] Q.S. Peng, Y.N. Cheng, W.B. Zhang, H. Fan, Q.H. Mao, P. Xu, circRNA_0000140 suppresses oral squamous cell carcinoma growth and metastasis by targeting miR-31 to inhibit Hippo signaling pathway, Cell Death Dis. 11 (2) (2020) 112.

[21] Y. Xi, Y. Shen, D. Wu, J. Zhang, C. Lin, L. Wang, C. Yu, B. Yu, W. Shen, CircBCAR3 accelerates esophageal cancer tumorigenesis and metastasis via sponging miR-27a-3p, Mol. Cancer 21 (1) (2022) 145.

[22] W. Yu, K. Ning, Q. Bai, J. Xiao, Circ_0001686 knockdown suppresses tumorigenesis and enhances radiosensitivity in esophagus cancer through regulating miR-876-5p/SPIN1 axis, Pathol. Res. Pract. 241 (2023), 154216.

[23] J. Wang, W. Zhu, G. Tao, W. Wang, Circular RNA circ-LRP6 facilitates Myc-driven tumorigenesis in esophageal squamous cell cancer, Bioengineered 11 (1) (2020) 932–938.

[24] Y. Zhang, X. Yuan, N. Yue, L. Wang, J. Liu, N. Dai, H. Yang, R. Fan, F. Zhou, hsa_circRNA6448-14 promotes carcinogenesis in esophageal squamous cell carcinoma, Aging (Albany NY) 12 (15) (2020) 15581–15602.

[25] C. Guo, J. Mi, H. Li, P. Su, H. Nie, Dysregulated circular RNAs as novel biomarkers in esophageal squamous cell carcinoma: a meta-analysis, Cancer Med. (2021).

[26] Q. Wang, H. Liu, Z. Liu, L. Yang, J. Zhou, X. Cao, H. Sun, Circ-SLC7A5, a potential prognostic circulating biomarker for detection of ESCC, Cancer Genet 240 (2020) 33–39.

[27] R. Zhong, Z. Chen, T. Mo, Z. Li, P. Zhang, Potential Role of circPVT1 as a proliferative factor and treatment target in esophageal carcinoma, Cancer Cell Int. 19 (2019) 267.

[28] W. Takaki, H. Konishi, K. Shoda, T. Arita, S. Kataoka, J. Shibamoto, H. Furuke, K. Takabatake, H. Shimizu, S. Komatsu, et al., Significance of circular FAT1 as a prognostic factor and tumor suppressor for esophageal squamous cell carcinoma, Ann. Surg Oncol. (2021).

[29] R. Zhao, P. Chen, C. Qu, J. Liang, Y. Cheng, Z. Sun, H. Tian, Circular RNA circTRPS1-2 inhibits the proliferation and migration of esophageal squamous cell carcinoma by reducing the production of ribosomes, Cell death discovery 9 (1) (2023) 5.

[30] H. Song, D. Tian, J. Sun, X. Mao, W. Kong, D. Xu, Y. Ji, B. Qiu, M. Zhan, J. Wang, circFAM120B functions as a tumor suppressor in esophageal squamous cell carcinoma via the miR-661/PPM1L axis and the PKR/p38 MAPK/EMT pathway, Cell Death Dis. 13 (4) (2022) 361.

[31] L. Fan, Q. Cao, J. Liu, J. Zhang, B. Li, Circular RNA profiling and its potential for esophageal squamous cell cancer diagnosis and prognosis, Mol. Cancer 18 (1) (2019) 16.

[32] C. Wang, S. Tan, J. Li, W.R. Liu, Y. Peng, W. Li, CircRNAs in lung cancer - biogenesis, function and clinical implication, Cancer Lett. 492 (2020) 106–115.

[33] J. Rong, Q. Wang, Y. Zhang, D. Zhu, H. Sun, W. Tang, R. Wang, W. Shi, X.F. Cao, Circ-DLG1 promotes the proliferation of esophageal squamous cell carcinoma, OncoTargets Ther. 11 (2018) 6723–6730.

[34] Q. Wang, Q. Zhang, H. Sun, W. Tang, L. Yang, Z. Xu, Z. Liu, H. Jin, X. Cao, Circ-TTC17 promotes proliferation and migration of esophageal squamous cell carcinoma, Dig. Dis. Sci. 64 (3) (2019) 751–758.

[35] W. Wang, D. Zhu, Z. Zhao, M. Sun, F. Wang, W. Li, J. Zhang, G. Jiang, RNA sequencing reveals the expression profiles of circRNA and identifies a four-circRNA signature acts as a prognostic marker in esophageal squamous cell carcinoma, Cancer Cell Int. 21 (1) (2021) 151.

[36] L. Fan, Q. Cao, J. Liu, J. Zhang, B. Li, Circular RNA profiling and its potential for esophageal squamous cell cancer diagnosis and prognosis, Mol. Cancer 18 (1) (2019) 16.

[37] H.D. Zhang, L.H. Jiang, D.W. Sun, J.C. Hou, Z.L. Ji, CircRNA: a novel type of biomarker for cancer, Breast Cancer 25 (1) (2018) 1–7.

[38] T. Yu, Y. Wang, Y. Fan, N. Fang, T. Wang, T. Xu, Y. Shu, CircRNAs in cancer metabolism: a review, J. Hematol. Oncol. 12 (1) (2019) 90.

[39] Z.H. Liu, S.Z. Yang, W.Y. Li, S.Y. Dong, S.Y. Zhou, S. Xu, circRNA_141539 can serve as an oncogenic factor in esophageal squamous cell carcinoma by sponging miR-4469 and activating CDK3 gene, Aging (Albany NY) 13 (8) (2021) 12179–12193.

[40] H. Cheng, W. Jiang, Z. Song, T. Li, Y. Li, L. Zhang, G. Wang, Circular RNA circLPAR3 facilitates esophageal squamous cell carcinoma progression through upregulating HMGB1 via sponging miR-375/miR-433, OncoTargets Ther. 13 (2020) 7759–7771.

[41] D. Zhang, C. Li, N. Cheng, L. Sun, X. Zhou, G. Pan, J. Zhao, CircAGFG1 acts as a sponge of miR-4306 to stimulate esophageal cancer progression by modulating MAPRE2 expression, Acta Histochem. 123 (7) (2021), 151776.

[42] L.Q. Wang, A.C. Deng, L. Zhao, Q. Li, M. Wang, Y. Zhang, MiR-1178-3p promotes the proliferation, migration and invasion of nasopharyngeal carcinoma Sune-1 cells by targeting STK4, J. Biol. Regul. Homeost. Agents 33 (2) (2019) 321–330.

[43] J. Bi, H. Liu, W. Dong, W. Xie, Q. He, Z. Cai, J. Huang, T. Lin, Circular RNA circ-ZKSCAN1 inhibits bladder cancer progression through miR-1178-3p/p21 axis and acts as a prognostic factor of recurrence, Mol. Cancer 18 (1) (2019) 133.

[44] Y. Ma, D. Yang, P. Guo, Circ_0000144 acts as a miR-1178-3p decoy to promote cell malignancy and angiogenesis by increasing YWHAH expression in papillary thyroid cancer, Journal of Otolaryngology - Head & Neck Surgery 51 (1) (2022) 28.

[45] X. Liu, J. Wu, D. Zhang, Z. Bing, J. Tian, M. Ni, X. Zhang, Z. Meng, S. Liu, Identification of potential key genes associated with the pathogenesis and prognosis of gastric cancer based on integrated bioinformatics analysis, Front. Genet. 9 (2018) 265.

[46] K.Z. Wu, X.H. Xu, C.P. Zhan, J. Li, J.L. Jiang, Identification of a nine-gene prognostic signature for gastric carcinoma using integrated bioinformatics analyses, World J. Gastrointest. Oncol. 12 (9) (2020) 975–991.

[47] R. Sun, Z. Lin, X. Wang, L. Liu, M. Huo, R. Zhang, J. Lin, C. Xiao, Y. Li, W. Zhu, et al., AADAC protects colorectal cancer liver colonization from ferroptosis through SLC7A11-dependent inhibition of lipid peroxidation, J. Exp. Clin. Cancer Res. 41 (1) (2022) 284.

[48] Q. Shi, M. Liu, S. Wang, P. Ding, Y. Wang, A novel pyroptosis-related model for prognostic prediction in esophageal squamous cell carcinoma: a bioinformatics analysis, J. Thorac. Dis. 15 (3) (2023) 1387–1397.

[49] N. Yi, H. Zhao, J. He, X. Xie, L. Liang, G. Zuo, M. Xiong, Y. Liang, T. Yi, Identification of potential biomarkers in Barrett's esophagus derived esophageal adenocarcinoma, Sci. Rep. 13 (1) (2023) 2345.